# Optimal Design of Nonlinear Hydraulic Engine Mount

**Young Kong Ahn**
*Research Center for Machine Parts and Material Processing, University of Ulsan, San 29, Muger 2-Dong, Ulsan 680-749, Korea*
**Jin Dae Song, Bo-Suk Yang***
*School of Mechanical Engineering, Pukyong National University, San 100, Yongdang-dong, Nam-gu, Busan 608-739, Korea*
**Kyoung Kwan Ahn**
*Research Center for Machine Parts and Material Processing, School of Mechanical & Automotive Engineering, University of Ulsan, Ulsan 680-749, Korea*
**Shin Morishita**
*Graduate School of Environment and Information Sciencies, Yokohama National University, 79-5 Tokiwadai, Hodogaya-ku, Yokohama 240-8501, Japan*

This paper shows that the performance of a nonlinear fluid engine mount can be improved by an optimal design process The property of a hydraulic mount with inertia track and decouplei differs according to the disturbance frequency range. Since the excitation amplitude is large at low excitation frequency range and is small at high excitation frequency range, mathematical model of the mount can be divided into two linear models One is a low frequency model and the other is a high frequency model The combination of the two models is very useful in the analysis of the mount and is used for the first time in the optimization of an engine mount in this paper Normally, the design of a fluid mount is based on a trial and error approach in industry because there are many design parameters In this study, a nonlinear mount was optimized to minimize the transmissibilities of the mount at the notch and the resonance frequencies for low and high-frequency models by a popular optimization technique of sequential quadratic programming (SQP) supported by MATLAB® subroutine. The results show that the performance of the mount can be greatly improved for the low and high frequencies ranges by the optimization method

**Key Words:** Fluid Mount, Nonlinear Fluid Mount, Optimal Design

## 1. Introduction

Engine mount is used to isolate noise and vibration generated by the engine with unbalanced disturbance at the high frequency range It is used to absorb engine vibration caused by shock excitation from a sudden acceleration, deceleration, braking or driving over uneven roads at low frequency range (Brach and Haddow, 1993, Yu et al, 2001) To effectively isolate the vibration and noise caused by the engine, low dynamic stiffness is used to isolate the forces transmitted to the structure However, high dynamic stiffness is required to absorb engine shake caused by shock excitation (Brach and Haddow, 1993, Yu et al., 2001, Flower, 1985).

Since rubber mounts are compact, cost-effective, maintenance free, the mounts have been successfully used for vehicle engine mounts for

* Corresponding Author,
**E-mail** bsyang@pknu ac kr
**TEL** +82-51-620-1604, **FAX** +82-51-620-1405
School of Mechanical Engineering, Pukyong National University, San 100, Yongdang-dong, Nam-gu, Busan 608-739, Korea (Manuscript **Received** April 22, 2004, **Revised** November 24, 2004)

many years However, the dynamic stiffness of rubber mounts increases according to the increase of disturbance frequency Therefore, stiffening the mount to achieve better connection results in poorer isolation at high frequency On the other hand, reducing the dynamic stiffness requires lower static stiffness and lead to weaker ability to hold the structures together To overcome some of the drawbacks of rubber mounts, fluid mounts are often used to provide a compromise between the static and dynamic requirements of the mount (Ahn et al , 2003 , Yu et al , 2001)

The resonance caused by fluid passing between the two compliant rubber chambers can either provide additional damping to the fundamental mount resonance, or create a tuned absorber effect to provide superior isolation at a single frequency depending on how the mount is designed The tuned absorber isolation effect by the fluid inertia results in a transmissibility and dynamic stiffness "notch" at which the transmissibility and the dynamic stiffness are low and high isolation effectiveness Therefore, fluid mounts can be designed to have higher static stiffness than rubber mounts at low frequency range and substantially higher isolation capability at the notch frequency

However, the transmissibility and dynamic stiffness of the fluid mount with an inertia track or with a simple orifice has an undesirable resonance peak because fluid inertia in the inertia track is greater than that of a comparable rubber mount (Yu et al , 2001) To resolve this problem, fluid mount with an inertia track and a decoupler was developed (Flower, 1985 , Yu et al , 2001) The property of the mount has amplitude or frequency range dependency, which means that the excitation amplitude is large at low excitation frequency range and small at high excitation frequency range The nonlinear property has been studied and mathematical models were proposed from the main phenomena of the mount (Kim and Singh, 1995 , Royston and Singh, 1997 , Geisberger et al , 2002 , Geisberger, 2000 , Colgate et al , 1995 , Singh et al , 1992 , Ushijima et al , 1988 , Lee and Choi, 1995 , Margolis and Wilson, 1997 , Jazer and Golnaraghi, 2002)

Optimizations of fluid mount and mounting system were attempted by some researches (Seto et al , 1991 , Tao, 2000 , Suresh et al , 1994) Their works on the optimization of the engine mount system show that the linear frequency dependent damping properties of the mount were considered, but the properties of the fluid mount such as nonlinear frequency and amplitude dependent stiffness and damping were not considered (Yu et al , 2001) Therefore, optimization to improve the performance of the mount by considering the nonlinear properties is shown in this study Two linear mathematical models related to the low and high frequency ranges and a popular optimization technique of sequential quadratic programming (SQP) supported by MATLAB® subroutine were used in the optimization process (Mathworks Inc, Version 2 1) Transmissibilities of the mount at resonance and notch frequencies were greatly reduced by the optimization method

## 2. Mathematical Model of a Nonlinear Fluid Mount with an Inertia Track and a Decoupler

The frequency range of engine disturbance with an engine speed range from 600 (or 760)-6000 rpm for a four cylinder is 20 (or 25)-200 Hz and for an eight-cylinder engine, the frequency range is double the frequency range of four cylinder (Brach and Haddow, 1993 , Yu et al , 2001) The frequency by shock excitation is below 30 Hz (Brach and Haddow, 1993) The nominal deformation amplitude of a mount in the range 20-200 Hz is less than 0 3 mm, while the amplitude in the range 1-30 Hz is greater than 0 3 mm

For a large amplitude caused by a shock excitation, the top compliance pumping action will cause the decoupler to contact the top or bottom of the cage, terminating liquid flow around it and sending the flow through the inertia track In this case, the static stiffness of the fluid mount is approximately equal to the static stiffness of the top rubber section because the bulge stiffness of the rubber below is very low (Yu et al , 2001)

As the frequency increases from 10 Hz (Kim and Singh, 1995), the fluid traveling through the

inertia track creates an additional damping, so that the dynamic stiffness increases until a maximum value is reached at the resonance frequency by the inertia track inertia. (Yu et al., 2001; Vahdati, 1999; Gau and Gotton, 1995; Ahn et al., 2003; Kim and Singh, 1995). Above the resonance frequency, the inertia track essentially close off. When this occurs, the stiffness of the mount is approximately equal to the sum of the rubber stiffness and the volumetric stiffness. At a high frequency and with small amplitude, the fluid travels around the decoupler instead of through the inertia track. Therefore, the resonance peak by the inertia track inertia decreases and also noise level decreases (Bernuchon, 1984).

The fluid mount with an inertia track and a decoupler is shown in Fig. 1. The nonlinear property of the mount changes according to the disturbance frequency range, which could be represented by two linear mathematical models by using the main mechanism of the mount. The two linear models are in good agreement with the practical behavior of the mount (Geisberger et al., 2002; Geisberger, 2000). The models are called as low-frequency model for the one and high-frequency model for the other. Dynamic stiffness of the low-frequency model represented as $K_L^*$ is shown in Eq. (1) which is also the same as that of a conventional fluid mount with an inertia track (Flower, 1985), while the dynamic stiffness of the high-frequency model represented as $K_H^*$ is shown in Eq. (2).

$$K_L^* = K_r + jB_r\omega + A_p^2 \frac{1 - C_2\omega(I_i\omega - jR_i)}{C_1\{1 - C_2\omega(I_i\omega - jR_i)\} + C_2} \quad (1)$$

$$K_H^* = K_r + jB_r\omega + \frac{A_p^2\{1 - C_2\omega(I_d\omega - jR_d)\} + A_pA_dC_2I_d\omega^2}{C_1\{1 - C_2\omega(I_d\omega^2 + jR_d)\} + C_2} \quad (2)$$

where $j = \sqrt{-1}$ and $\omega$ is excitation frequency in rad/s, $K_r$ and $B_r$ are the rubber stiffness and damping coefficients in the top chamber, respectively, $A_p$ is the effective piston area. $A_d$ is the average cross-sectional area of the decoupler and $I_i$ and $I_d$ are the inertia track and decoupler inertia, respectively. $R_i$ and $R_d$ are the resistance in the inertia track and decoupler respectively, and $C_1$ and $C_2$ are compliance in the top and bottom chambers, respectively. Compliance is defined as the ratio of a volume change to pressure change caused by bulge of rubber. Volumetric stiffness is expressed by the reciprocal of the compliance. Equations (1) and (2) are very useful in preventing unnecessary complexity in the optimization of the mount. In Eqs. (3) ~ (6), the real part of the dynamic stiffness, $K'$, represents the stiffness property of the mount, and the imaginary part, $K''$ indicates its damping property.

$$K_L' = K_r + \frac{A_p^2(D_1/C_1 + (C_2I_i\omega^2 - 1)D_3)}{D_1 + D_3^2} \quad (3)$$

$$K_L'' = B_r + \frac{A_p^2C_2^2R_i\omega}{D_1 + D_3^2} \quad (4)$$

$$K_H' = K_r + \frac{A_p\left[\frac{A_pD_2}{C_1} - \{A_p + C_2I_d\omega^2(A_d - A_p)\}D_4\right]}{D_2 + D_4^2} \quad (5)$$

$$K_H'' = B_r + \frac{A_pC_2^2R_d\omega(A_p - A_dC_1I_d\omega^2)}{D_2 + D_4^2} \quad (6)$$

where

$$D_1 = (C_1C_2R_i\omega)^2,\ D_2 = (C_1C_2R_d\omega)^2$$
$$D_3 = C_1(C_2I_i\omega^2 - 1) - C_2$$
$$D_4 = C_1(C_2I_d\omega^2 - 1) - C_2$$

and subscripts $L$ and $H$ mean low and high-frequency models, respectively. Transmissibility is

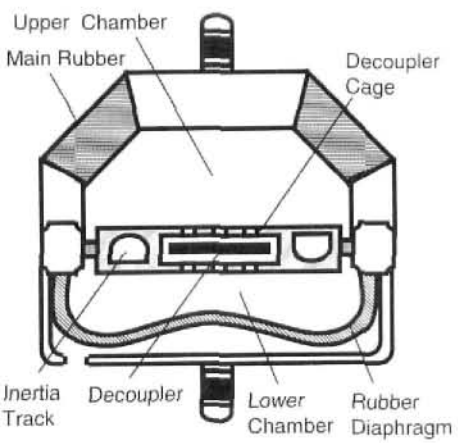


**Fig. 1** Schematic diagram of a hydraulic engine mount with inertia track and decoupler

useful in assessing the isolation effectiveness of the mount and can be obtained from the real and imaginary parts of the dynamic stiffness

$$T_{RD}=\frac{X-Y}{Y}=\frac{M\omega^2}{\sqrt{(K_L'-M\omega^2)^2+K_L''^2}} \tag{7}$$

$$T_F=\frac{F_t}{F_e}=\sqrt{\frac{(K_H'^2+K_H''^2)}{(K_H'-M\omega^2)^2+K_H''^2}} \tag{8}$$

where $T_{RD}$ and $T_F$ are relative displacement and force transmissibilities respectively for low and high-frequency models, $F_t$ and $F_e$ are transmitted and input forces respectively, and $M$ is mass of the engine The relative displacement for low frequency and large amplitude need to be investigated since it is related to the motion of the engine on the mounts relative to the chassis which needs to be controlled Furthermore, the forces transmitted to the chassis should be examined since the forces result in the transmission of acoustical noise to the passenger compartment

Assuming that there is no damping (i e , $B_e=B_v=B_d=0$), the notch and resonance frequencies shown in Fig 2 generally selected by the mount designer can be obtained for the dynamic stiffness, relative displacement and force transmissibilities from their zeros and poles

$$\omega_{DLR}=\sqrt{\frac{C_1+C_2}{C_1C_2I_t}} \tag{9}$$

$$\omega_{DHR}=\sqrt{\frac{C_1+C_2}{C_1C_2I_d}} \tag{10}$$

$$\omega_{TL1}=\sqrt{\frac{P_1-\sqrt{(P_1^2-4C_1C_2I_tMP_2)}}{2C_1C_2I_tM}} \tag{11}$$

$$\omega_{TL2}=\sqrt{\frac{P_1+\sqrt{(P_1^2-4C_1C_2I_tMP_2)}}{2C_1C_2I_tM}} \tag{12}$$

$$\omega_{TH1}=\sqrt{\frac{P_3-\sqrt{(P_3^2-4C_1C_2I_dMP_2)}}{2C_1C_2I_dM}} \tag{13}$$

$$\omega_{TH2}=\sqrt{\frac{P_3+\sqrt{(P_3^2-4C_1C_2I_dMP_2)}}{2C_1C_2I_dM}} \tag{14}$$

$$\omega_{DLN}=\sqrt{\frac{A_p^2+K_r(C_1+C_2)}{(C_2I_t(A_p^2+C_1K_r))}} \tag{15}$$

$$\omega_{TLN}=\sqrt{\frac{C_1+C_2}{C_1C_2I_t}} \tag{16}$$

$$\omega_{THN}=\omega_{DHN}=\sqrt{\frac{A_p^2+K_r(C_1+C_2)}{C_2I_d(A_p^2-A_dA_p+C_1K_r)}} \tag{17}$$

where

$$P_1=C_2I_t(A_p^2+C_1K_r)+M(C_1+C_2)$$

$$P_2=A_p^2+K_r(C_1+C_2)$$

$$P_3=C_2I_d(A_p^2-A_pA_d+C_1K_r)+M(C_1+C_2)$$

and subscripts $D$ and $T$ mean dynamic stiffness and transmissibility respectively, subscripts $R$ and

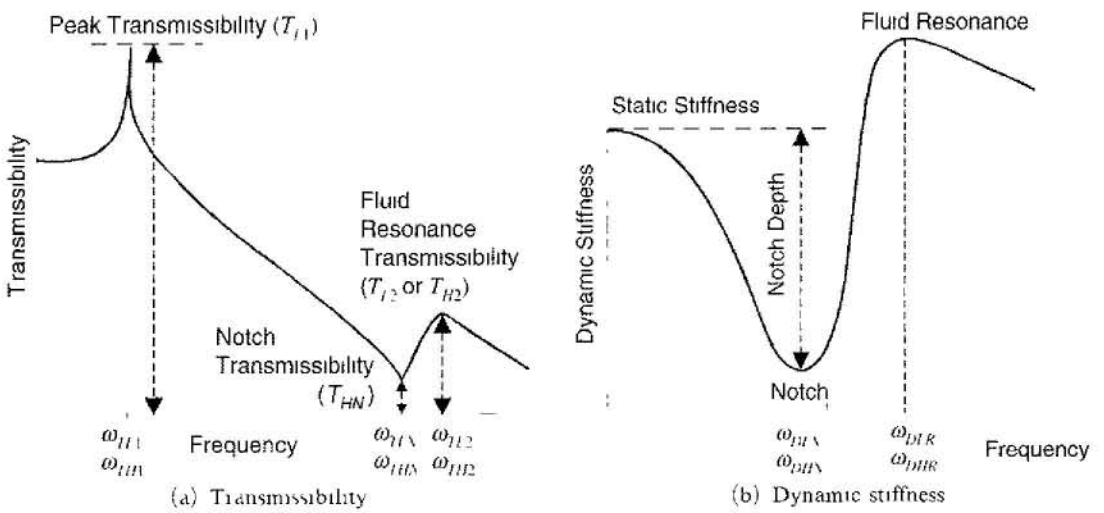


**Fig. 2** Notch and resonance frequencies of the fluid mount

$N$ represent resonance and notch frequencies respectively, subscripts 1 and 2 mean the first and second resonance frequencies, respectively. The second resonance is caused by the fluid inertia The notch frequency of the transmissibility of the high-frequency model is exactly the same as that of the dynamic stiffness

## 4. Optimal Design of the Nonlinear Fluid Mount with an Inertia Track and a Decoupler

SQP is employed as the optimization technique to minimize the transmissibilities of the fluid mount with an inertia track and a decoupler The objective function $f(X)$ is constructed as follows,

$$f(X)=\alpha_1\beta_1 T_{L1}(X)+\alpha_2\beta_2 T_{L2}(X) +\alpha_3\beta_3 T_{HN}(X)+\alpha_4\beta_4 T_{H2}(X) \quad (18)$$

Where $\alpha_1-\alpha_4$ are weight factors, $\beta_2$ $(=1/T_{L1}(X_0))$, $\beta_2$ $(=1/T_{L2}(X_0))$, $\beta 3$ $(=1/T_{HN}(X_0))$ and $\beta 4$ $(=1/T_{H2}(X_0))$ are scale factors, $T_{L1}$ and $T_{L2}$ are the transmissibilities at the first and second resonance frequencies respectively for low-frequency model, and $T_{HN}$ and $T_{H2}$ are the force transmissibilities at the notch and second resonance frequencies respectively for high-frequency model These frequencies can be calculated from Eqs (9)~(16) To obtain an effective isolation for the mount in the low and high frequency ranges, the objective function was combined with the low and high-frequency models and was minimized The design parameters which can greatly affect the isolation effectiveness were taken as the design variables as follow

$$X=\{A_p\ I_d\ I_t\ R_d\ R_t\ K_r\ C_1\}^T \quad (19)$$

subject to

$$0.7X_0<X<1.3X_0 \quad (20)$$

where $X_0$ is the original design parameters listed in Table 1 These different cases are used to improve the isolation performance of the mount in the optimization process These cases are defined as follows,

$$\left.\begin{array}{ll} \text{Case 1} & \alpha_1=1,\ \alpha_2=1,\ \alpha_3=1 \\ & \text{with } \omega_{THN} \text{ constraint, } \alpha_4=1 \\ \text{Case 2} & \alpha_1=1,\ \alpha_2=1,\ \alpha_3=0 \\ & \text{without } \omega_{THN} \text{ constraint, } \alpha_4=1 \\ \text{Case 3} & \alpha_1=1,\ \alpha_2=1,\ \alpha_3=1 \\ & \text{without } \omega_{THN} \text{ constraint, } \alpha_4=1 \end{array}\right\} \quad (21)$$

The parameters in Case 1 with constraint for the notch frequency location are set to minimize the transmissibilities at resonance frequencies and are also used to minimize the transmissibility at notch frequency selected by the mount designer The constraint for location of the notch frequency $\omega_{THN}$ is defined as follows,

$$\omega_{THN}-\pi<\omega_{THN}<\omega_{THN}+\pi \quad (22)$$

where $\pi$ is 3 14159 and $\omega_{THN}$ is notch frequency obtained from Eq (17) using the design parameters listed in Table 1 The notch frequency is closely related with the main speed of the engine. Furthermore, the resonance peaks of the optimized mount for the low and high frequency models are constrained to be below 5% of those of the original mount. The optimization conditions for Case 2 are set to reduce only the transmissibilities at resonance frequencies and not take the transmissibility at notch frequency into account The parameter conditions for Case 3 were used to minimize the resonance peaks and the transmissibility at notch frequency and does not take the notch frequency location into account

**Table 1** Mount parameters used in numerical simulation

| Parameters | Original value, $X_0$ |
|---|---|
| $A_p$ | $2.5\times10^{-3}$ m$^2$ |
| $A_d$ | $6.6\times10^{-4}$ m$^2$ |
| $I_t$ | $3.8\times10^{6}$ N·s$^2$/m$^5$ |
| $I_d$ | $7.5\times10^{4}$ N·s$^2$/m$^5$ |
| $R_t$ | $1.05\times10^{8}$ N·s/m$^5$ |
| $R_d$ | $1.17\times10^{7}$ N·s/m$^5$ |
| $C_1$ | $3.0\times10^{-11}$ m$^5$/N |
| $C_2$ | $2.6\times10^{-9}$ m$^5$/N |
| $K_r$ | $2.25\times10^{5}$ N/m |
| $B_r$ | 100 N·s/m |
| $M$ | 62 kg |

The optimization results for Case 1 are shown in Fig. 3. Since the optimization results of SQP depend on the initial design values, optimization is investigated using three different initial design values. original values are listed in Table 1, minimum and maximum values are in the design

**Table 2** Optimal Parameters of optimized mounts

| Design variables | Original variables | Case 1 | | Case 2 | Case 3 |
|---|---|---|---|---|---|
| | | Var ratio % | | Var ratio % | Var ratio % |
| | | Min & orig | Max | Min, Orig & Max | Min, Orig & Max |
| $A_p$ | $2.5\times10^{-3}$ m$^2$ | 13.7 | −12.65 | 8.82 | −2.41 |
| $I_d$ | $7.5\times10^{4}$ N·s$^2$/m$^5$ | −30.00 | 19.21 | −30.00 | −30.00 |
| $I_t$ | $3.8\times10^{6}$ N·s$^2$/m$^5$ | −30.00 | 9.38 | −30.00 | −30.00 |
| $R_d$ | $1.17\times10^{7}$ N·s/m$^5$ | −14.08 | 28.25 | 30.00 | 21.98 |
| $R_t$ | $1.05\times10^{8}$ N·s/m$^5$ | 30.00 | 30.00 | 30.00 | 30.00 |
| $K_r$ | $2.25\times10^{5}$ N/m | −30.00 | −28.81 | −30.00 | −30.00 |
| $C_t$ | $3.0\times10^{-11}$ m$^5$/N | 30.00 | −16.48 | 30.00 | −30.00 |
| Values of $f(X)$ | | 2.92 | 3.43 | 1.87 | 2.69 |

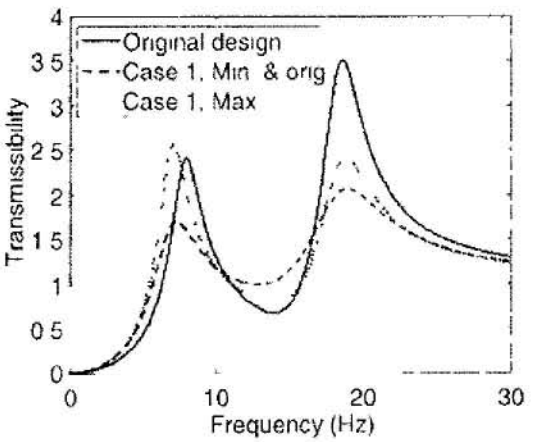


(a) Transmissibility of low-frequency model

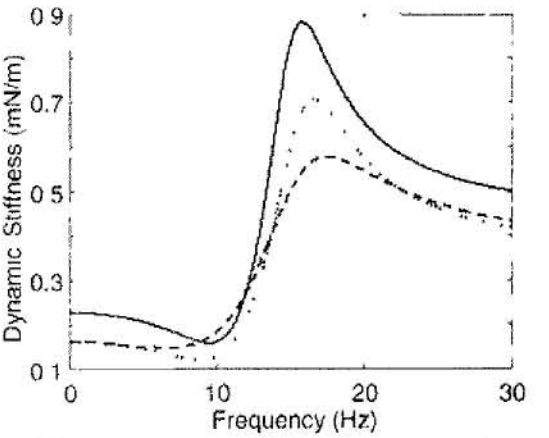


(b) Dynamic stiffness of low-frequency model

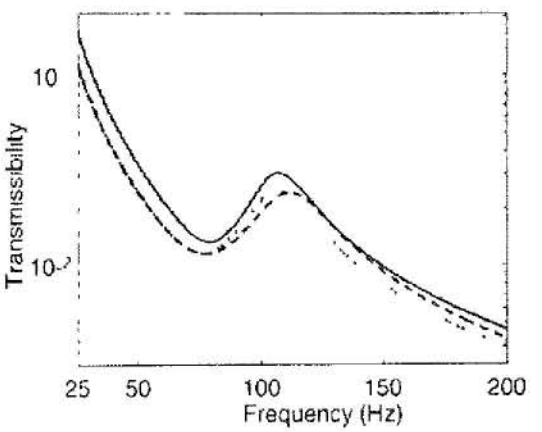


(c) Transmissibility of high-frequency model

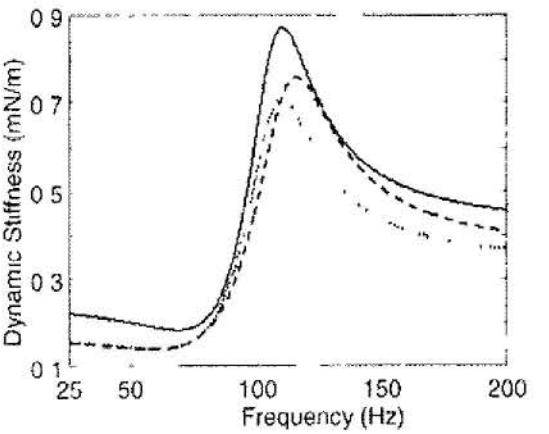


(d) Dynamic stiffness of high-frequency model

**Fig. 3** Optimized mounts without the notch frequency constraint, Case 1

variable boundary shown in Eq (20). These three initial values are represented in Fig. 3 by subscripts min., orig. and max.. The optimization result obtained from the initial minimum value is the same as that from original, and the value of the objective function listed in Table 2 is reduced more than that from the initial maximum value. Even though the results are depend on the initial design values, global optimization of the mount can be easily obtained by the trial and error approach because the objective function for the optimization is not too complex.

Figure 4 show optimization results obtained for Case 1 with the initial minimum and original values, Case 2 and 3. The results for Cases 2 and 3 without constraint for the notch frequency do not depend on the initial design value. The results for Case 1 is similar to those for Case 2, but the transmissibility at the second resonance peaks for Case 1 is higher than that for Case 2 because Case 2 does not take transmissibility at the notch frequency into account. However, the transmissibilities for Case 1 at the first and notch frequencies for the low frequency model and at the notch frequency for the high frequency model are lower than those for Case 2.

Variation of volumetric stiffness of the optimized mount for Case 3 listed in Table 2 increased, which is opposite tendency to those for Case 1 and 2. Therefore, the notch and the resonance frequencies caused by fluid inertia for Case 3 increased and their transmissibilities decreased by decreasing the fluid inertia of the inertia track and the decoupler. The isolation effec-

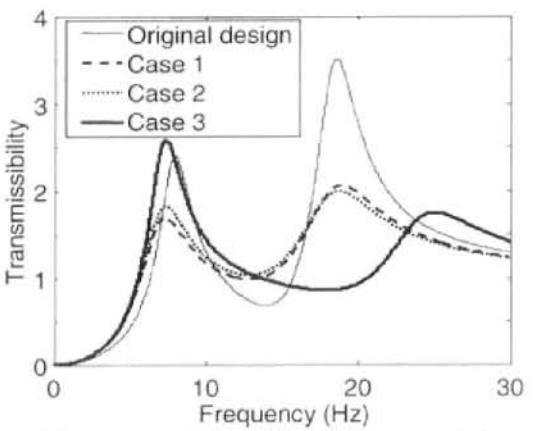


(a) Transmissibility of low-frequency model

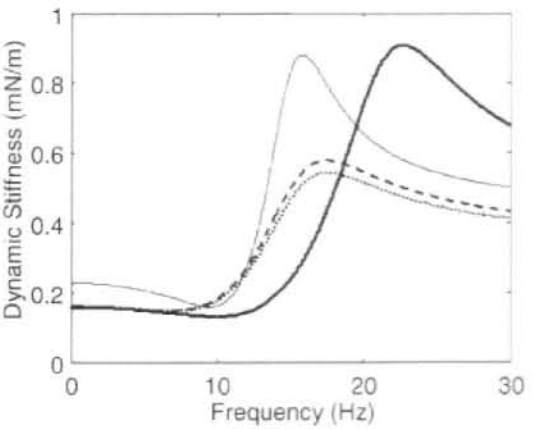


(b) Dynamic stiffness of low-frequency model

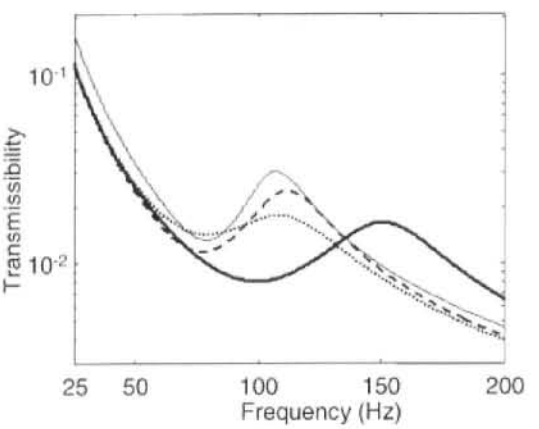


(c) Transmissibility of high-frequency model

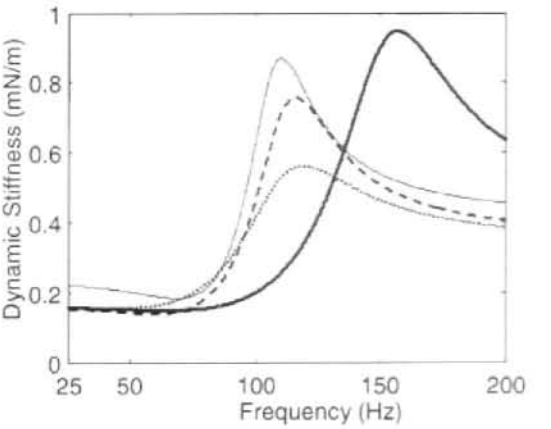


(d) Dynamic stiffness of high-frequency model

**Fig. 4** Optimized mounts

tiveness for the high frequency range is greatly improved by increasing the first resonance peaks because of the decreased dynamic stiffness

The mount performance of optimized mount for Case 3 is better than those for Case 1 and 2 in the high frequency range, while those for Case 1 and 2 are better than that for Case 3 in the low frequency range Even though dynamic stiffness is a useful measure in assessing the isolation effectiveness of the mount, the optimization results show that the transmissibility curve in evaluating the isolation effectiveness is more useful than the dynamic stiffness curve because transmissibility curve has information for the first resonance peaks but dynamic stiffness curve does not Furthermore, the transmissibility curve shows a different tendency from the dynamic stiffness at the second resonance frequency

**Table 3** Transmissibility and dynamic stiffness of original mount and optimized mounts at resonance and notch frequencies of their own

| | | Transmissibility | | | | Dynamic Stiffness | | | |
|---|---|---|---|---|---|---|---|---|---|
| | | Low-frequency model [Mag /freq (Hz)] | | High-frequency model [Mag /freq (Hz)] | | Low-frequency model [Mag /freq (Hz)] | | High-frequency model [Mag /freq (Hz)] | |
| | | $T_{L1}$ ($\omega_{TL1}$) | $T_{L2}$ ($\omega_{TL2}$) | $T_{HN}$ ($\omega_{THN}$) | $T_{H2}$ ($\omega_{TH2}$) | $K^*_{LN}$ ($\omega_{DLN}$) | $K^*_{LR}$ ($\omega_{DLR}$) | $K^*_{HN}$ ($\omega_{DHN}$) | $K^*_{HR}$ ($\omega_{DHR}$) |
| Original Design | | 2 403 (7 99) | 3 502 (18 60) | 0 013 (79 43) | 0 031 (107 49) | 0 158 (9 55) | 0 881 (15 79) | 0 183 (69 19) | 0 870 (110 44) |
| Case 1 | Min & Orig | −33 06% (6 81) | −41 29% (18 78) | −12 66% (79 90) | −20 69% (112 36) | −6 21% (6 79) | −34 35% (17 50) | −22 94% (60 09) | −12 73% (116 11) |
| | Max | 5 00% (6 91) | −32 38% (18 46) | −11 34% (79 42) | −18 48% (107 11) | −23 59% (8 98) | −19 53% (16 59) | −22 81% (61 23) | −18 53% (110 41) |
| Case 2 (Min , Orig & Max ) | | −27 53% (6 89) | −43 35% (18 46) | 7 45% (81 81) | −41 98% (112 36) | −6 51% (7 01) | −38 27% (17 54) | −14 24% (41 59) | −35 55% (119 37) |
| Case 3 (Min , Orig & Max ) | | 5 00% (7 13) | −51 26% (24 19) | −39 06% (100 75) | −46 12% (152 47) | −17 67% (10 03) | 3 09% (22 69) | −18 07% (64 90) | 9 00% (157 13) |

**Table 4** Transmissibility and dynamic stiffness of optimized mounts and original mount at resonance and notch frequencies of the original mount

| | | Transmissibility | | | | Dynamic Stiffness | | | |
|---|---|---|---|---|---|---|---|---|---|
| | | Low frequency model [Mag /freq (Hz)] | | High-frequency model [Mag /freq (Hz)] | | Low-frequency model [Mag /freq (Hz)] | | High-frequency model [Mag /freq (Hz)] | |
| | | $T_{L1}$ ($\omega_{TL1}$) | $T_{L2}$ ($\omega_{TL2}$) | $T_{HN}$ ($\omega_{THN}$) | $T_{H2}$ ($\omega_{TH2}$) | $K^*_{LN}$ ($\omega_{DLN}$) | $K^*_{LR}$ ($\omega_{DLR}$) | $K^*_{HN}$ ($\omega_{DHN}$) | $K^*_{HR}$ ($\omega_{DHR}$) |
| Original Design | | 2 403 (7 99) | 3 502 (18 60) | 0 013 (79 43) | 0 031 (107 49) | 0 158 (9 55) | 0 881 (15 79) | 0 183 (69 19) | 0 870 (110 44) |
| Case 1 | Min & Orig | −33 51% (7 99) | −41 47% (18 60) | −12 88% (79 43) | −23 88% (107 49) | 8 19% (9 55) | −38 31% (15 79) | −19 97% (69 19) | −18 05% (110 44) |
| | Max | −15 63% (7 99) | −31 72% (18 60) | −11 35% (79 43) | −18 53% (107 49) | −22 42% (9 55) | −22 51% (15 79) | −20 20% (69 19) | −18 53% (110 44) |
| Case 2 (Min , Orig & Max ) | | −28 09% (7 99) | −43 24% (18 60) | 7 23% (79 43) | −41 30% (107 49) | 4 95% (9 55) | −42 14% (15 79) | −1 85% (69 19) | −39 29% (110 44) |
| Case 3 (Min , Orig & Max ) | | −2 50% (7 99) | −75 47% (18 60) | −24 30% (79 43) | −72 65% (107 49) | −17 38% (9 55) | −67 40% (15 79) | −17 91% (69 19) | −70 57% (110 44) |

Optimization results shown in Figs 3 and 4 are summarized in Tables 3 and 4 In Table 3, transmissibility and dynamic stiffness of the optimized mounts are compared with those of original mount at their own resonance and notch frequencies The optimized ones are expressed as percentage of the ratio of the optimized mounts and the original mount On the other hand, in Table 4, transmissibility and dynamic stiffness of the optimized and original mounts at resonance and notch frequencies of the original mount are shown In table 3, transmissibility and dynamic stiffness of optimized ones are expressed as percentage of the ratio of those of optimized mounts to those of original mount

## 5. Conclusions

Optimization of a nonlinear fluid mount with an inertia track and a decoupler was firstly conducted The design parameters of the mount could be optimized without unnecessary complexity by using linear low and high-frequency models and a popular optimization technique of SQP supported by MATLAB® subroutine This study shows that the performance of a mount can be greatly improved in the initial mount design stage by the simple optimization process Results of the case study are as follows

Transmissibilities of the optimized mounts at the first and second resonance frequencies in the low frequency range were reduced by about 33 51% and 41 47% respectively for Case 1 with the initial minimum and original values, by about 28 08% and 43 24% for Case 2, by about 2 50% and 75 47% for Case 3

Transmissibilities of the optimized mounts at the second resonance and the notch frequencies in the high frequency range were reduced by about 12 88% and 23 88% respectively for Case 1 with the initial minimum and original values, by about 7 23% and 41 30% for Case 2, by about 24 30% and 72 65% for Case 3

The mount performance of optimized mount for Case 3 is better than those for Case 1 and 2 in the high frequency range, while those for Case 1 and 2 are better than that for Case 3 in the low frequency range

## Acknowledgment

This work was supported in part by the Korea Science and Engineering Foundation (KOSEF) through the Research Center for Machine Parts and Materials Processing (ReMM) at University of Ulsan

## References

Ahn, Y K, Song, J D and Yang, B S, 2003, "Optimal Design of Engine Mount Using an Artificial Life Algorithm," *Journal of Sound and Vibration*, Vol 261, No 2, pp 309~328

Bernuchon, M, 1984, "A New Generation of Engine Mount," *SAE Techanical Paper* #840259

Brach, R M and Haddow, A G, 1993, "On the Dynamic Response of Hydraulic Engine Mounts," *SAE Techanical Paper* #931321

Colgate, J, Chang, T, Chiou, C, Liu, K and Kerr, M., 1995, "Modeling of a Hydraulic Engine Mount Focusing on Response to Sinusoidal and Composite Excitations," *Journal of Sound and Vibration*, Vol. 184, pp. 503~528

Flower, W C, 1985, "Understanding Hydraulic Mounts for Improved Vehicle Noise Vibration and Ride Qualities," *SAE Techanical Paper* #850975

Gau, S J and Cotton J D, 1995, "Experimental Study and Modeling of Hydraulic Mount and Engine System," *SAE Techanical Paper* #951348

Geisberger, A, 2000, "Hydraulic Engine Mount Modeling, Parameter Identification and Experimental Validation," *Master's thesis, University of Waterloo*, Canada

Geisberger, A, Khajepour, A and Golnaraghi, F, 2002, "Nonlinear Modeling of Hydraulic Mounts Theory and Experiment," *Journal of Sound and Vibration*, Vol 249, No 2, pp 371~397

Jazer, G N and Golnaraghi, M F, 2002, "Nonlinear Modeling, Experimental Verification, and Theoretical Analysis of a Hydraulic Engine Mount," *Journal of Vibration and Control*, Vol

8, pp 87~116

Kim, G and Singh, R, 1995, "A study of passive and Adaptive Hydraulic Engine Mount Systems with Emphasis on Non-linear Characteristics," *Journal of Sound and Vibration*, Vol 179, pp 427~453

Lee, K and Choi, Y, 1995, "Performance Analysis of Hydraulic Engine Mount by Using Bond Graph Method," *SAE Techanical Paper* #951347

Margolis, D and Wilson, R, 1997, "Modeling Simulation and Physical Understanding of Hydromounts," *Master's Thesis, University of California*

Miller, L R, Ahmadian, M, Nobles, C M and Swanson, D A, 1995, "Modeling and Performance of an Experimental Active Vibration Isolator," *Trans ASME Journal of Vibration and Acoustics*, Vol 117, No 3A, pp 272~278

Royston, T and Singh, R, 1997, "Study of Nonlinear hydraulic Engine Mounts Focusing on Decoupler Modeling and Design," *SAE Techanical Paper* #971936

Seto, K, Sawatari, K, Nagamatsu, A, Ishihama, M and Doi, K, 1991, "Optimum Design Method for Hydraulic Mount," *SAE Techanical Paper* #911055

Singh, R, Kim, G and Ravindra, P V, 1992, "Linear Analysis of Automotive Hydro-Mechanical Mount with Emphasis on Decoupler Characteristics," *Journal of Sound and Vibration*, Vol 158, No 2, pp 219~243

Suresh, N, Shankar, S and Bokil, V, 1994, "Develpoment of Idealistic Hydromount Characteristics to Minimize Engine Induced Vibrations Using Unconstrained Minimization," *SAE Paper* #941741

Swanson, D A, 1993, "Active Engine Mounts for Vehicles," *SAE Paper* #932432

Tao, J S, Liu, G R and Lam, K Y, 2000, "Design Optimization of Marine Engine-Mount System," *Journal of Sound and Vibration*, Vol 235, No 3, pp 477~494

The Mathworks Inc Version 2 1 (Release 12), *Optimization Toolbox for Use with Matlab*

Ushijima, T, Takano, K and Kojima, H, 1988, "High Performance Hydraulic Mount for Improving Vehicle Noise and Vibration," *SAE Techanical Paper* #880073

Vahdati, N, 1999, "Incorporation of TVAs on Soft Structures to Improve Vibration Isolation," *Asia-Pacific Vibration Conference* '99, Singapore, December 1999

Yang, B S and Song, J D, 2001, "Enhanced Artificial Life Algorithm for Fast and Accurate Optimization Search," *Proceedings of Asia-Pacific Vibration Conference*, pp 732~736

Yu, Y, Peelamedu, S M, Naganathan, N G and Dukkipati, R V, 2001, "Automotive Vehicle Engine Mounting Systems A Survey," *Trans ASME, J Dynamic Systems, Measurement, and Control*, Vol 123, pp 186~194